

Range Doppler Detection for automotive FMCW Radars

Volker Winkler

DICE GmbH & Co KG

Majority owned by Infineon Technologies
Freistaedterstrasse 400, 4040 Linz, Austria
volker.winkler@infineon.com

Abstract—The FMCW-Radar-Principle is widely used for automotive radar systems. The basic idea for FMCW-Radars is to generate a linear frequency ramp as transmit signal. The difference frequency between the transmitted and received signal is determined after downconversion. In order to detect range and velocity together, the information, extracted from one frequency ramp, is not enough, because it is ambiguous. Several subsequent ramps have to be generated to remove the ambiguity between the frequency portion produced by range and the doppler frequency. In this paper two methods are presented to perform this basic signal processing step. The two methods have the Fast Fourier Transform as basic calculation step in common, but the number of FFTs and their length are different. The requirements on bandwidth for the IF-Hardware and A/D-Converters are also determined by the algorithm for Range-Doppler-Detection. The CFAR(Constant False Alarm Rate)-Algorithm for target detection must also be adapted to the chosen method. Both methods have been verified with a 24 GHz radar prototype. The Radar-Frontend has been built with a newly developed SiGe-Radar-Chipset on Infineon's B7HF200-Process with a transition frequency of 200 GHz.

I. PROTOTYPING HARDWARE

The Front-End consists of one TX-Chip and RX-Chip, each in a TSLP-16-Package. The TX-Chip comes with an VCO, integrated divider and two output buffers. One output buffer is dedicated for LO Distribution, the other one feeds the transmit antenna. Fig. 1 shows the TX-Board with two ratrace baluns to convert the differential outputs of the two buffers to single-ended microstrip line. The RX-Chip (left side on fig. 1) has two receive paths in parallel with a Low Noise Amplifier as input stage and a subsequent active Gilbert Cell Mixer. The two receive paths allow an angle detection according to the phase monopulse principle. The prototype was configured as a short range system with a sweep bandwidth $B = 1$ GHz from 24 GHz to 25 GHz. Fig. 2 shows a complete system diagram.

II. FMCW RADAR EQUATIONS

In the following the equations for the FMCW Radar principle are presented in order to derive the implemented algorithms. The basic idea in FMCW is to generate a linear frequency ramp. The transmit frequency for one ramp with bandwidth B and duration T between $[-T/2; T/2]$ can be expressed as:

$$f_T(t) = f_c + \frac{B}{T}t \quad (1)$$

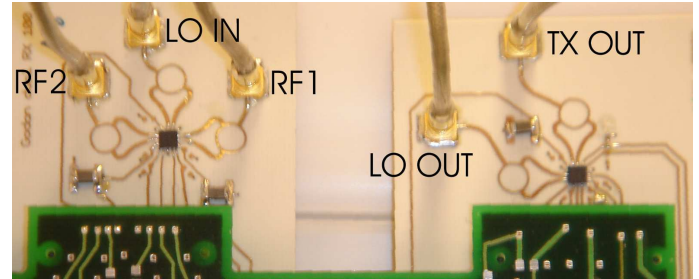


Fig. 1. RX-Board(left) and TX-Board(right) connected to Motherboard with IF-Hardware

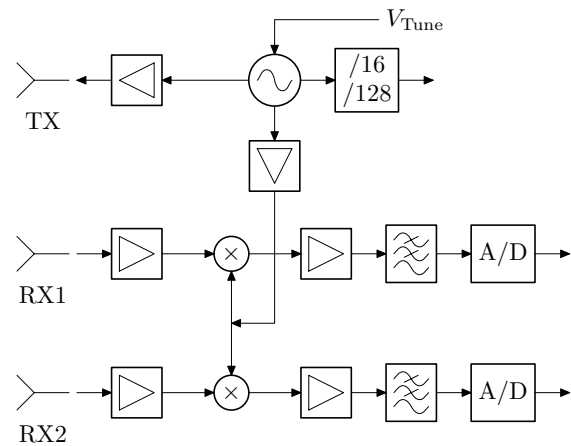


Fig. 2. System Diagram

The phase $\varphi_T(t)$ of the transmitted signal $\cos(\varphi_T(t))$ becomes after integration:

$$\begin{aligned} \varphi_T(t) &= 2\pi \int_{-T/2}^t f_T(t) dt \\ &= 2\pi \left(f_c t + \frac{1}{2} \cdot \frac{B}{T} t^2 \right) \Big|_{-T/2}^t \\ &= 2\pi \left(f_c t + \frac{1}{2} \cdot \frac{B}{T} t^2 \right) - \varphi_{T0} \end{aligned} \quad (2)$$

The phase of the downconverted signal $\Delta\varphi(t) = \varphi_T(t) - \varphi_T(t - \tau)$ is:

$$\Delta\varphi(t) = 2\pi \left(f_c \tau + \frac{B}{T} t \tau - \frac{B}{2T} \tau^2 \right) \quad (3)$$

τ is the delay between the transmitted and received signal of one target. The last term in the equation above can be neglected because $\tau/T \ll 1$. For calculation of the delay $\tau = 2(R + v \cdot t)/c$ a target at distance R with constant velocity v is assumed. This leads to:

$$\Delta\varphi(t) = 2\pi \left[\frac{2f_c R}{c} + \left(\frac{2f_c \cdot v}{c} + \frac{2B \cdot R}{Tc} \right) t + \frac{2B \cdot v}{T \cdot c} t^2 \right] \quad (4)$$

The last term is called Range-Doppler-Coupling and can be neglected again:

$$\Delta\varphi(t) = 2\pi \left[\frac{2f_c R}{c} + \left(\frac{2f_c \cdot v}{c} + \frac{2B \cdot R}{Tc} \right) t \right] \quad (5)$$

The generated frequency is therefore:

$$f_{IF} = \frac{2f_c \cdot v}{c} + \frac{2B \cdot R}{Tc} \quad (6)$$

The received signal $s_{IF} = \cos(\Delta\varphi(t))$ is sampled with an interval T_A , the samples are multiplied with a window function $w(n)$ and a zero padding is performed, before a Fast Fourier Transform with the resulting samples is done. The spectrum is symmetric, because the input signal is real. The complex baseband signal can be obtained by $s_{IF}(t) + i \cdot H\{s_{IF}(t)\}$, where $H\{\dots\}$ denotes the Hilbert transformation:

$$s_B(n) = A \cdot w(n) e^{i \cdot 2\pi \left[\frac{2f_c R}{c} + \left(\frac{2f_c \cdot v}{c} + \frac{2B \cdot R}{Tc} \right) T_A n \right]} \quad (7)$$

In order to simplify the following equations the window function isn't taken into account and A is set to one, which doesn't cause the loss of generality.

III. DETECTION BASED ON A TWO DIMENSIONAL FFT

For this algorithm, which has been described in [5], L frequency ramps have to be generated after another like shown in fig. 3. The ramp repetition interval is called T_{RRI} in the

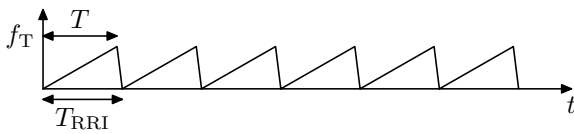


Fig. 3. Ramp Generation for 2D-FFT

following. The resulting IF-Signal can be expressed as:

$$s_{IF,2D}(t) = \sum_{l=0}^{L-1} e^{i \cdot 2\pi \left[\frac{2f_c (R + v \cdot T_{RRI} \cdot l)}{c} + \left(\frac{2f_c \cdot v}{c} + \frac{2B \cdot (R + v \cdot T_{RRI} \cdot l)}{Tc} \right) \cdot t \right]} \cdot \text{rect} \left(\frac{t - l \cdot T_{RRI}}{T} \right) \quad (8)$$

The frequency increase can also be neglected, because the movement during the measurement is short compared to the

distance R .

$$s_{IF,2D}(t) = e^{i \cdot 4\pi f_c \cdot R/c} \sum_{l=0}^{L-1} e^{i \cdot 2\pi \left[\frac{2f_c \cdot v \cdot T_{RRI} \cdot l}{c} + \left(\frac{2f_c \cdot v}{c} + \frac{2B \cdot R}{Tc} \right) \cdot t \right]} \cdot \text{rect} \left(\frac{t - l \cdot T_{RRI}}{T} \right) \quad (9)$$

The signal is sampled with $f_A = 1/T_A$ during each ramp and a two dimensional fourier transformation is performed:

$$S_{2D}(k, p) = e^{i \cdot 4\pi f_c \cdot R/c} \sum_{l=0}^{L-1} \sum_{n=0}^{N-1} e^{i \cdot 4\pi \frac{v T_{RRI} \cdot f_c}{c} l} e^{i \cdot 2\pi \left[\left(\frac{2f_c \cdot v}{c} + \frac{2B \cdot R}{Tc} \right) \cdot n \cdot T_A \right]} \cdot e^{-i \cdot 2\pi \left(\frac{l \cdot p}{L_Z} + \frac{n \cdot k}{N_Z} \right)} \quad (10)$$

N_Z and L_Z is the matrix size of S_{2D} after zero-padding. Reordering the equation above leads to:

$$S_{2D}(k, p) = e^{i \cdot 4\pi f_c \cdot R/c} \sum_{l=0}^{L-1} e^{i \cdot 4\pi \frac{v T_{RRI} \cdot f_c}{c} l} \left[\sum_{n=0}^{N-1} e^{i \cdot 2\pi \left[\left(\frac{2f_c \cdot v}{c} + \frac{2B \cdot R}{Tc} \right) \cdot n \cdot T_A - \frac{n \cdot k}{N_Z} \right]} \right] \cdot e^{-i \cdot 2\pi \frac{l \cdot p}{L_Z}} \quad (11)$$

From this equation it becomes obvious that a peak appears at the following position:

$$k = \left(\frac{2f_c \cdot v}{c} + \frac{2B \cdot R}{Tc} \right) T_A \cdot N_Z \quad (12)$$

$$p = \frac{2v \cdot f_c \cdot T_{RRI} \cdot L}{c} = f_D \cdot T_{RRI} \cdot L_Z \quad (13)$$

In order to fulfill the sampling theorem, the following constraint for the maximum doppler frequency $f_{D,max}$ must be met:

$$f_{D,max} < \frac{1}{2 \cdot T_{RRI}} \quad (14)$$

It can be easily seen that the velocity resolution Δv is determined by the overall measurement time $T_{RRI} \cdot L$:

$$\Delta v = \frac{c}{2f_c \cdot T_{RRI} \cdot L} \quad (15)$$

The straight-forward way to implement the algorithm is to perform a FFT for each single ramp. For each range gate the doppler spectrum must be calculated. The target detection can be done with a simple CFAR algorithm directly in the doppler spectrum, because the number of targets in one doppler spectrum is low in practical cases. For the prototype setup the following parameters have been chosen: Ramps $L = 32$, Ramp Duration $T = 200\mu s$, Ramp Repetition Interval $T_{RRI} = 220\mu s$, Sampling Frequency $f_A = 2.5$ MHz. Therefore $N = 500 = T \cdot f_A$ samples are generated per ramp. The samples are multiplied with a blackman window and after zero-padding to $N_Z = 1024$ samples the FFT for each ramp is calculated. A measurement in the laboratory is depicted in fig. 4, where the displayed range is limited to 7 m. In the upper part the time domain signal and the logarithmic

FFT amplitude of each ramp is shown, while the detected targets can be seen in the lower part. There's the logarithmic amplitude of the doppler spectrum shown where the velocity is drawn at the top of each bin. The target detection was performed in the doppler spectrum with a Cell Averaging-CFAR(see [2]) and local maxima search. For calculation of the doppler spectrum a blackman window was applied again and zero-padding to $L_Z = 128$ was used. This measurement has

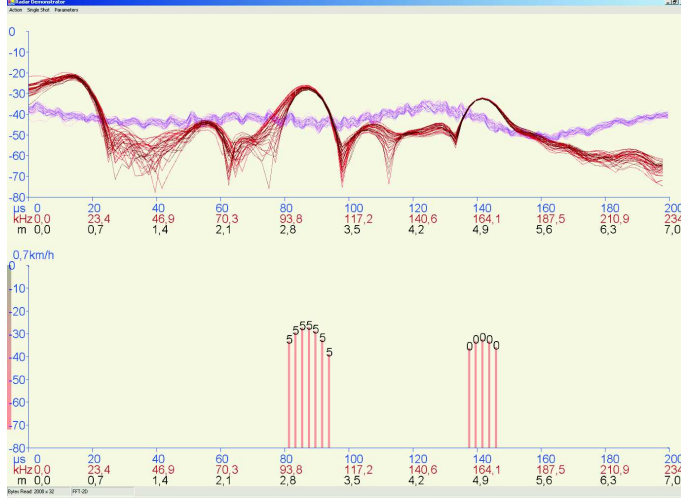


Fig. 4. Detection with 2D-FFT: Moving Target at 3 m, Static Target at 5 m

been done with a TX-Chip with an integrated divider of 128 and a subsequent external divider of 10. The resulting signal around 19 MHz becomes a LVTTTL-Logic-Signal with the help of voltage comparator. The frequency of this signal can be easily determined by the used FPGA. The VCO frequency is directly set by a D/A-converter that sets the voltage at the Tune-Input of the VCO. The tuning law of the VCO is determined by setting a number of different voltages. After this static calibration a frequency ramp can be generated by calculating the values for the D/A-converter with the measured tuning law.

IV. DETECTION WITH SUBSEQUENTS RAMPS OF DIFFERENT SLOPES

This method uses slow ramps with different slopes like shown in fig. 5. All Chirps occupy the bandwidth B . For the

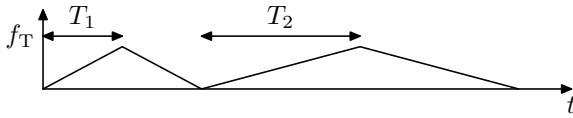


Fig. 5. Ramp Generation with different slopes

first up-chirp and down-chirp with ramp duration T_1 the IF-Signal is sampled with frequency $f_{A,1} = 1/T_{A,1}$. The number of samples is therefore $N = T_1/T_{A,1}$. The sampling rate of the subsequent chirps with T_2 is chosen according to the ramp duration:

$$\frac{T_{A,1}}{T_{A,2}} = \frac{T_1}{T_2} = \frac{f_{A,2}}{f_{A,1}} = M \quad (16)$$

The Ratio M is an integer, e. g. $M = 2$. If the movement during the measurement time is small, one target creates the following frequencies for each ramp according to equ. 6:

$$\begin{aligned} f_{1,\text{up}} &= \frac{2B \cdot R}{T_1 c} + \frac{2f_c \cdot v}{c} \\ f_{1,\text{down}} &= \frac{2B \cdot R}{T_1 c} - \frac{2f_c \cdot v}{c} \\ f_{2,\text{up}} &= \frac{2B \cdot R}{T_2 c} + \frac{2f_c \cdot v}{c} \\ f_{2,\text{down}} &= \frac{2B \cdot R}{T_2 c} - \frac{2f_c \cdot v}{c} \end{aligned} \quad (17)$$

Taking equ. 11 into account, a peak around the following integer position in each FFT Spectrum occurs:

$$\begin{aligned} k_{1,\text{up}} &= \left[\frac{2B \cdot R}{cT_1} + \frac{2f_c \cdot v}{c} \right] T_{A,1} \cdot N_Z \\ k_{1,\text{down}} &= \left[\frac{2B \cdot R}{cT_1} - \frac{2f_c \cdot v}{c} \right] T_{A,1} \cdot N_Z \\ k_{2,\text{up}} &= \left[\frac{2B \cdot R}{cT_1 \cdot M} + \frac{2f_c \cdot v}{c} \right] T_{A,1} \cdot M \cdot N_Z \\ k_{2,\text{down}} &= \left[\frac{2B \cdot R}{cT_1 \cdot M} - \frac{2f_c \cdot v}{c} \right] T_{A,1} \cdot M \cdot N_Z \end{aligned} \quad (18)$$

For each range gate position $k_{1,\text{up}}$ in the FFT spectrum the corresponding discrete positions $k_{1,\text{down}}, k_{2,\text{up}}$ and $k_{2,\text{down}}$ must be searched where the maximum velocity $\pm v_{\text{max}}$ must be covered. The following equation states the issue clearly, where x_r and x_v are the assumed range position and velocity increment:

$$\begin{aligned} k_{1,\text{up}} &= \left[\frac{R}{\Delta R} + \frac{v}{\Delta v} \right] \frac{N_Z}{N} = x_r + x_v \\ k_{1,\text{down}} &= \left[\frac{R}{\Delta R} - \frac{v}{\Delta v} \right] \frac{N_Z}{N} = x_r - x_v \\ k_{2,\text{up}} &= \left[\frac{R}{\Delta R} + \frac{v \cdot M}{\Delta v} \right] \frac{N_Z}{N} = x_r + M \cdot x_v \\ k_{2,\text{down}} &= \left[\frac{R}{\Delta R} - \frac{v \cdot M}{\Delta v} \right] \frac{N_Z}{N} = x_r - M \cdot x_v \end{aligned} \quad (19)$$

The range resolution ΔR is determined by the bandwidth, Δv is the velocity resolution of the shortest ramp. After the FFT a CFAR is performed on each single ramp. Hence the search needs only to be done with the positions that have exceeded their CFAR threshold. So the calculation effort is quite relaxed. The exact implementation of the algorithm will be dependent of the used device, e.g. FPGA or DSP. Because there can be many peaks in one FFT spectrum, the CFAR-Algorithm must be of high quality which leads to the corresponding computational effort. The number of FFTs is low compared to the two dimensional method and equals the number of used ramps.

If one wants to use a fractional value instead of an integer value M , an interpolation in the spectrum can be done: A simple approach is to do a linear interpolation with the surrounding values under the constraint that the surrounding values are also greater than the CFAR threshold.

Fig. 6 and fig. 7 show a laboratory scene with a static and moving target. The logarithmic FFT amplitude and CFAR thresholds are depicted in the upper part, the lower part shows the detected targets. The separation of the peaks due to the doppler frequency can be clearly seen. The shown amplitude of the detected targets is the average of the amplitudes at the corresponding positions $k_{1,up}$, $k_{1,down}$, $k_{2,up}$ and $k_{2,down}$. The measurement parameters have been: Ramp Duration $T_1 = 2048 \mu s$ and $T_2 = 4096 \mu s$, Sampling Rate $f_{A,1} = 500 \text{ kHz}$ and $f_{A,1} = 250 \text{ kHz}$. The resulting $N = 1024$ samples per ramp are multiplied with a blackman window and a FFT is performed after zero-padding to $N_Z = 2048$ Samples. An Ordered Statistics-CFAR is used for target detection on each ramp. With the presented algorithm the final targets are extracted under the additional constraint that the target positions are local maxima in the doppler range. For this measurement a TX-Chip with an integrated divider of 16 has been used, the divided VCO-Signal at 1.5 GHz is fed to a PLL Synthesizer whose reference signal is modulated to generate the desired frequency chirps. The algorithm can be

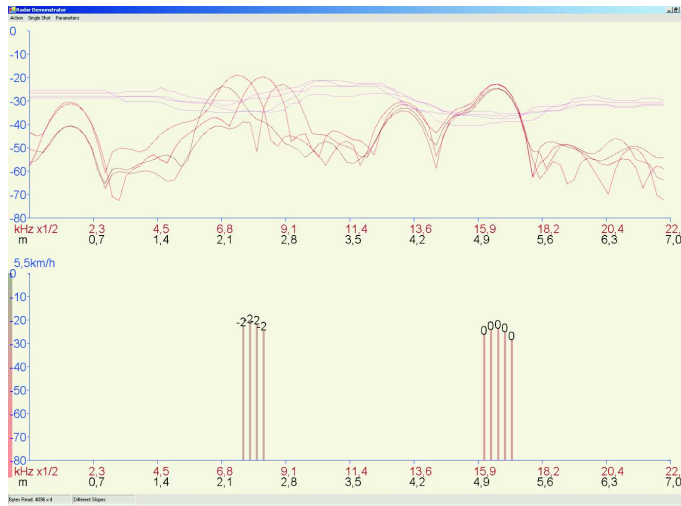


Fig. 6. Detection with different slopes: Moving Target

generalised to an arbitrary number of ramps. The problem of range doppler detection has been addressed in [4] and [3] for FSCW-Radar (FS=Frequency Stepped) and FMCW and in [6] and [7] for FMCW. The problem of range doppler detection has been described as intersectioning process in the R-v-diagram (see equ. 17): Every beat frequency leads to a line in the R-v-diagram with different slope. For one target the intersection point of lines with different slopes must be searched. If there is an additional intersection, a ghost target is detected accidentally. This is especially a problem for distributed targets. The number of required targets to produce one ghost target is equal to the number of used ramps.

V. CONCLUSIONS AND OUTLOOK

For the algorithm based on a two dimensional FFT fast ramps have to be generated to fulfill the sampling theorem for the highest doppler frequency. This leads to IF-Frequencies in

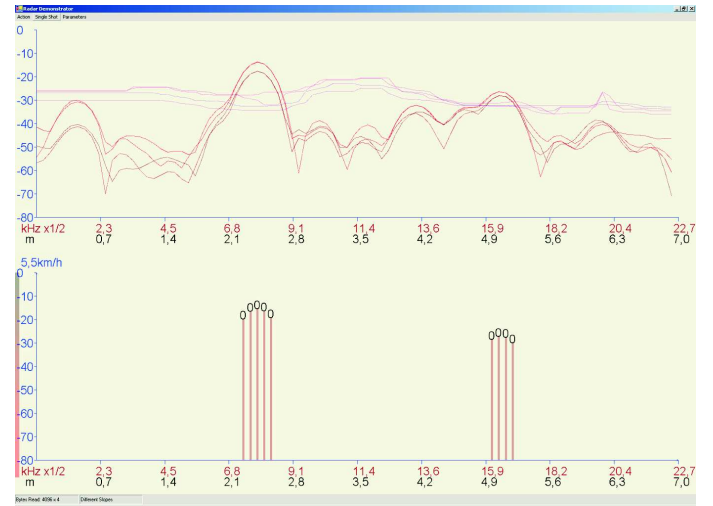


Fig. 7. Detection with different slopes: Static Target

the range of several megahertz. The ramp generation can be easily implemented with a D/A-converter that feeds the tune input of the VCO. The algorithm with different slopes requires slow ramps in order to achieve a certain velocity resolution. In that case the IF-frequencies are in the range of a few hundred kilohertz. The slow ramp generation allows the use of a Phase Locked Loop for ramp generation. In the future we want to implement the algorithms on an embedded device and test it in real traffic scenarios combined with angle detection according to the phase monopulse principle.

The radar will also be tested with an improved version of the chipset which is currently under production.

ACKNOWLEDGMENTS

I want to thank my colleagues G. Haider und Yang S. for their great efforts in doing the chip design. The used patch antenna array in the prototype setup was designed by R. Feger from the Institute for Communications and Information Engineering at the Johannes Kepler University Linz.

REFERENCES

- [1] Rohling H. *Radar CFAR Thresholding in Clutter and Multiple Target Situations* (IEEE Transactions on Aerospace and Electronic Systems, AES-19, July 1983, pp. 608-621)
- [2] Ludloff A. *Praxiswissen Radar und Radarsignalverarbeitung* (Vieweg, 1998)
- [3] Meinecke, Marc Michael; Rohling H. *Combination of LFM CW and FSK Modulation Principles for Automotive Radar Systems* (German Radar Symposium GRS 2000)
- [4] Meinecke, Marc Michael; Rohling H. *Waveform Design Principles for Automotive Radar Systems* (German Radar Symposium GRS 2000)
- [5] Stove, A.G.; *Linear FMCW radar techniques* (Radar and Signal Processing, IEE Proceedings F, Volume 139, Issue 5, Oct. 1992, pp. 343-350)
- [6] Folster, F.; Rohling H.; Lubbert U. *An Automotive radar network based on 77GHz FMCW sensors* (Radar Conference, 2005 IEEE International, 9-12 May 2005, pp. 871-876)
- [7] Mende, R.; Rohling H.; *A High-Performance AICC radar sensor-concept and results with an experimental vehicle* (Radar 97 (Conf. Publ. No. 449), 14.-16. Oct 1997, pp. 21-25)